Cardiac Overexpression of Melusin Protects From Dilated Cardiomyopathy Due to Long-Standing Pressure Overload

Marika De Acetis, Antonella Notte, Federica Accornero, Giulio Selvetella, Mara Brancaccio, Carmine Vecchione, Mauro Sbroggiò, Federica Collino, Beniamina Pacchioni, Gerolamo Lanfranchi, Alessandra Aretini, Roberta Ferretti, Angelo Maffei, Fiorella Altruda, Lorenzo Silengo, Guido Tarone and Giuseppe Lembo

Circulation Research 2005, 96:1087-1094: originally published online April 28, 2005
doi: 10.1161/01.RES.0000168028.36081.e0
Circulation Research is published by the American Heart Association. 7272 Greenville Avenue, Dallas, TX 72514
 Print ISSN: 0009-7330. Online ISSN: 1524-4571

Cardiac Overexpression of Melusin Protects From Dilated Cardiomyopathy Due to Long-Standing Pressure Overload

Marika De Acetis,* Antonella Notte,* Federica Accornero,* Giulio Selvetella, Mara Brancaccio, Carmine Vecchione, Mauro Sbroggiò, Federica Collino, Beniamina Pacchioni, Gerolamo Lanfranchi, Alessandra Aretini, Roberta Ferretti, Angelo Maffei, Fiorella Altruda, Lorenzo Silengo, Guido Tarone, Giuseppe Lembo

Abstract—We have previously shown that genetic ablation of melusin, a muscle specific β 1 integrin interacting protein, accelerates left ventricle (LV) dilation and heart failure in response to pressure overload.

Here we show that melusin expression was increased during compensated cardiac hypertrophy in mice subjected to 1 week pressure overload, but returned to basal levels in LV that have undergone dilation after 12 weeks of pressure overload. To better understand the role of melusin in cardiac remodeling, we overexpressed melusin in heart of transgenic mice. Echocardiography analysis indicated that melusin over-expression induced a mild cardiac hypertrophy in basal conditions (30% increase in interventricular septum thickness) with no obvious structural and functional alterations. After prolonged pressure overload (12 weeks), melusin overexpressing hearts underwent further hypertrophy retaining concentric LV remodeling and full contractile function, whereas wild-type LV showed pronounced chamber dilation with an impaired contractility. Analysis of signaling pathways indicated that melusin overexpression induced increased basal phosphorylation of GSK3β and ERK1/2. Moreover, AKT, GSK3β and ERK1/2 were hyper-phosphorylated on pressure overload in melusin overexpressing compared with wild-type mice. In addition, after 12 weeks of pressure overload LV of melusin overexpressing mice showed a very low level of cardiomyocyte apoptosis and stromal tissue deposition, as well as increased capillary density compared with wild-type. These results demonstrate that melusin overexpression allows prolonged concentric compensatory hypertrophy and protects against the transition toward cardiac dilation and failure in response to long-standing pressure overload. **(*Circ Res*. 2005;96:1087-1094.)**

Key Words: melusin ■ cardiac hypertrophy ■ heart failure ■ signal transduction ■ fibrosis

Mechanical stretching imposed on cardiac walls by hemodynamic overload generated by several cardiovascular diseases, such as aortic stenosis, hypertension and myocardial infarction, triggers left ventricular hypertrophy (LVH), a process aimed to increase cardiac pumping function and normalize wall stress. This response is achieved via signaling pathways, which trigger increased synthesis of sarcomeric proteins and growth of cardiomyocyte mass. In addition, LVH is accompanied by release and secretion of neurohumoral mediators, growth factors, and cytokines that, contribute to the growth of cardiomyocytes, as well as blood vessels and interstitial connective tissue. Consistent with this general picture, a variety of different signaling pathways have been implicated in the hypertrophic growth of cardiac muscle.[1,2]

Although LVH provides increased contractile power, several clinical and experimental studies have demonstrated that cardiac hypertrophy is frequently associated with an increased risk of heart failure. Following chronic pressure overload, in fact, compensatory hypertrophy can evolve to decompensated hypertrophy with cardiac dilation and loss of contractile function, representing the typical features of heart failure. This unfavorable evolution can be accounted for by several causes, including abnormal accumulation of stromal tissue, poor development of capillary vascular bed, myocyte apoptosis, inadequate cardiomyocyte growth, and defective Ca^{2+} cycling.[2] The molecular mechanisms responsible for this transition are still poorly defined and identification of genes and signaling pathways involved represents a major challenge of molecular cardiology.

Original received October 4, 2004; revision received April 19, 2005; accepted April 19, 2005.

From the Department of Genetics, Biology (M.DA, F.A., M.B., M.S., F.C., R.F., F.A., L.S., G.T.), and Biochemistry, Turin University, Turin; Dept. of Angiocardioneurology (A.N., G.S., C.V., A.A., A.M., G.L.), I.R.C.C.S. "Neuromed", Pozzilli (IS); Experimental Medicine Research Center (F.A., L.S., G.T.), San Giovanni Battista Hospital, Turin; Dept. of Experimental Medicine and Pathology (G. Lembo), "La Sapienza" University of Rome; Dept. of Biology and CRIBI Biotechnology Centre (B.P., G. Lanfranchi).

*These authors contributed equally to this work.

Correspondence to Guido Tarone, Dept. of Genetics, Biology, and Biochemistry, Turin University, Via Santena, 5bis, 10126 Turin, Italy. E-mail guido.tarone@unito.it; or Giuseppe Lembo, Department of Angiocardioneurology, I.R.C.C.S. "Neuromed", 86077 Pozzilli (IS), Italy. E-mail lembo@neuromed.it

Circulation Research **is available at http://www.circresaha.org** **DOI: 10.1161/01.RES.0000168028.36081.e0**

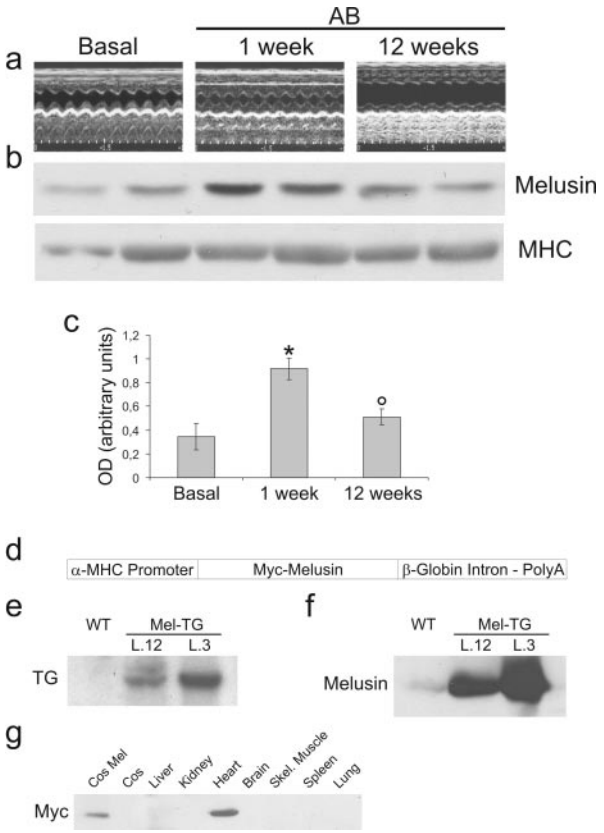

Figure 1. Melusin expression in LV after AB and characterization of Mel-TG mice. Echocardiography of WT mice in basal conditions and after 1 or 12 weeks AB (a). Western blot on LV proteins with melusin, or myosin heavy chain (MHC) antibodies as loading control (b). Densitometric analysis of melusin expression, relative to total protein loading (n=5 per group) (c). DNA construct used for generation of transgenic mice (d). Two independent Mel-TG lines were analyzed (L.12 and L.3). Southern blot of genomic DNA from WT and Mel-TG mice probed with human melusin cDNA (e). Western blot of proteins from WT and Mel-TG LV probed with melusin antibodies (f). Western blot of different tissues from L.12 transgenic line probed with Myc antibodies specific for the transgenic protein. COS cells transfected with myc-tagged melusin cDNA (Cos mel) as positive control (g). (*): $P<0.05$ versus basal conditions, (°): $P<0.05$ versus 1 week AB.

We have previously identified melusin as a new muscle-specific protein binding to the cytoplasmic domain of integrins[3] and acting as mechanical stretch sensor. Targeted inactivation of melusin gene in mice caused impaired LVH with accelerated development of dilated cardiomyopathy in response to chronic pressure overload.[4]

Here we report that cardiac selective overexpression of melusin in transgenic mice allows retainment of concentric compensatory hypertrophy and proper contractile function in conditions of prolonged pressure overload leading to LV dilation and contractile dysfunction in control wild-type (WT).

Materials and Methods

Generation of Transgenic Mice

Alpha-MHC promoter[5] was cloned upstream the myc-tagged human melusin cDNA followed by β-globin intron and poly-A (Figure 1D). The DNA construct described previously was microinjected in FVB fertilized eggs and transgenic integration was confirmed by Southern blot (Figure 1E). The use of animals was in compliance with European Community guidelines and was approved by the Animal Care and Use Committee of Turin University.

LV Pressure Overload

A chronic pressure overload was imposed to the LV through transverse aortic banding (AB), as previously described.[4] Systolic pressure gradient (SPG) was measured by selective cannulation of left and right carotid arteries during the hemodynamic analysis at 12 weeks of AB.[4]

LV Echocardiographic and Hemodynamic Analysis

Conscious blood pressure and heart rate were measured in unrestrained conditions by radiotelemetry as previously described.[6] Serial echocardiographic evaluations were assessed in mice in basal conditions and during chronic pressure overload (4, 8, and 12 weeks after banding) as described.[4] Hemodynamic measurements were performed in anesthetized aortic-banded and sham-operated mice after 12 weeks from AB, as described.[4]

Histological Analysis

Histological analysis was performed as described.[4] Fibrosis was quantified by Picrosirius red followed by ImageProPlus software analysis. Apoptotic cells were detected by TUNEL. Capillaries were identified by anti von Willebrand factor antibodies (Sigma).

Isolation of Adult Cardiomyocytes and Morphometric Analysis

Cardiomyocytes were enzymatically dissociated from hearts as described.[7] Freshly isolated cardiomyocytes were photographed at 20x phase contrast and cell areas were measured using ImageProPlus software.

Embryonic Cardiomyocyte Isolation and Transduction

Ventricular cardiomyocytes were prepared from Sprague-Dawley rat hearts as described.[8] Final cultures contained >95% cardiomyocytes as determined by actin staining.

Lentiviral vector coding for myc-tagged human melusin, and a control vector coding for GFP, were prepared as described.[9] Forty-eight hours after plating, cardiomyocyte were incubated overnight with lentivirus. Infection efficiency was ≈80%. After washing, cells were further incubated for 72 hours with or without 50 μmol/L MEK-1 inhibitor (PD98059, Calbiochem) or 20 μmol/L AKT inhibitor (1L-6-hydroxymethyl-chiro-inositol-2(R)-2-O-methyl-3-O-octadecylcarbonate, Calbiochem). Cells were fixed and stained with FITC–labeled phalloidin (Sigma) or subjected to Western blot analysis.

Northern and Western Blot Analysis

Northern blots with LV RNA were performed as described[4] and probed with atrial natriuretic factor (ANF) and alpha-skeletal actin (SkA) radiolabeled probes. Western blots on LV protein extracts were performed as described.[4] Polyclonal antibodies to melusin were prepared as described.[3]

Transcriptome Analysis

Gene expression profile was performed on a mouse microarray platform with a collection of 13,443 70mer oligonucleotides (Qiagen-Operon, version 1.1). Preparation of the microarray, RNA labeling, hybridization and detection of differentially expressed transcripts are described in online supplementary information at http://www.circresaha.org.

Statistical Analysis

Results are presented as mean±S.E. Differences between groups were compared using 2-way ANOVA followed by Bonferroni *post-hoc* test. A value of $P<0.05$ was considered significant.

TABLE 1. Haemodynamic Parameters in Sham- and AB-Operated Mel-TG and WT Control Mice

	WT		Mel-TG	
	Sham n=6	AB 12w n=7	Sham n=6	AB 12w n=7
BW, g	30.6±0.6	29.3±0.3	31.2±0.7	28.4±0.7
HR	350±9	322±22	362±9	344±24
SPG, mm Hg	—	77.5±3.2	—	81.2±3.1
EDV, μL	95.2±43.7	118±2[b]	91.3±4.2	96.0±5.8[a]
ESV, μL	64±6.5	93.5±2.5[b]	60.5±4	60±5[a]
ESP, mm Hg	88.8±7.2	155.6±9.2[b]	93.7±4.3	161.2±8.0[b]
EDP, mm Hg	6.9±2.3	15.2±3.5[b]	6.8±1	4.5±1[a]
dP/dT_{max}	6077±601	4017±504[b]	7102±612	7377±577[a]
dP/dT_{min}	−4544±443	−3366±413[b]	−5343±797	−3697±316[b]
EDPVR	0.13±0.03	0.17±0.07	0.12±0.09	0.08±0.04
τ(Glanz) (ms)	17.6±1.8	25.5±5	18.8±4	25.7±4
Emax	2.6±0.7	1.8±0.6	2.5±1.3	5.4±1.6[a]

[a]$P<0.05$ vs WT.

[b]$P<0.05$ vs basal conditions.

BW, body wt; HR, heart rate; SPG, systolic pressure gradient; ESV, end-systolic volume; EDV, end-diastolic volume; ESP, end-systolic pressure; EDP, end-diastolic pressure; dp/dt_{max}, maximal rate of pressure development; Emax, maximum chamber elasticity; dp/dt_{min}, maximal rate of pressure decay; τ(Glanz), monoexponential time constant of relaxation; EDPVR, end diastolic pressure-volume relationship.

Results

Melusin Expression in Pressure Overloaded Hearts

To investigate whether melusin expression is modified by pressure overload, WT were subjected to AB for different times. Whereas after 1 week LV showed a concentric hypertrophic remodeling, at 12 weeks the chamber was clearly dilated (Figure 1a). Melusin expression increased by 2.6-fold over basal ($P<0.05$ in 5 hearts) in the first week of AB (Figure 1b,c). However, after 12 weeks of AB, melusin expression in LV was decreased as compared with 1 week of AB ($P<0.05$, n=5) and not significantly different from basal levels. Thus, melusin expression is regulated during the LV remodeling induced by chronic pressure overload.

These data, together with the finding that inactivation of melusin gene in mice causes premature evolution toward dilated cardiomyopathy in response to pressure overload,[4] led us to test whether forced melusin expression can prevent cardiac dilation in conditions of chronic pressure overload.

Generation of Mice Overexpressing Melusin in Heart

Two lines (L.3 and L.12) of transgenic FVB mice selectively expressing myc-tagged melusin transgene in the heart were selected (Mel-TG) (Figure 1G). Melusin expression was increased ≈15-fold and 8-fold in L.3 and L.12 lines respectively compared with WT littermates as detected by western blot (Figure 1F).

Transgenic mice were born in a normal Mendelian distribution, excluding lethal developmental abnormalities. They exhibit normal reproductive rate and gender distribution and did not demonstrate any difference in longevity over 2 years. All experiments reported were performed with male mice and both transgenic lines displayed comparable phenotype, ruling out the possibility that the alterations detected are due to insertional mutagenesis.

Melusin Overexpressing Mice Show LVH in Basal Conditions

Mel-TG mice exhibited a slight LVH as compared with WT (LVW/BW: 3.12±0.11 versus 2.84±0.08, n=11 per group, $P<0.05$), even with comparable systolic and diastolic blood pressure (SBP: 108±4 versus 110±3; DBP: 84±1 versus 85±1 mm Hg) and heart rate (579±50 versus 552±37 bpm) as detected by radiotelemetric measurements in conscious mice. Furthermore, LV contractile function and diastolic relaxation, evaluated by dP/dt max and by dP/dt min and τ Glantz, respectively, were also comparable between Mel-TG and WT mice (Table 1).

However, echocardiography showed a different basal LV geometry between the 2 mouse strains (Table 2). Both interventricular septum and LV posterior wall thickness were significantly increased in Mel-TG as compared with WT, resulting in significantly higher relative wall thickness. LV histological analysis indicated that myocyte cross-sectional areas were ≈30% higher in Mel-TG hearts compared with WT (Figure 2A,B). This level of hypertrophy was confirmed by analysis of cardiomyocytes isolated from adult hearts (Figure 2C,D). No histological signs of stromal tissue deposition were observed, suggesting that LVH in Mel-TG mice can be ascribed to increased cardiomyocyte size.

Therefore, in basal conditions, melusin overexpression does not affect cardiac function, but induces a significant concentric LVH.

In addition, Northern blot analysis showed increased ANF, but reduced SkA expression in Mel-TG LV (Figure 2E,F) indicating a specific pattern of LVH.

TABLE 2. Echocardiographic Parameters in Basal Conditions and After AB in WT and Mel-TG Mice

	WT				Mel-TG			
	Basal n=11	AB 4w n=11	AB 8w n=11	AB 12w n=10	Basal n=8	AB 4w n=8	AB 8w n=8	AB 12w n=7
BW, g	26.4±0.5	27.6±0.7[b]	28.7±0.5[bc]	29.5±0.3	26.3±0.4	27.0±0.4[b]	28.4±0.6[bc]	28.4±0.7[b]
HR, bpm	624±9	625±10	608±10	621±12	622±10	615±10	623±13	619±13
LVEDD, mm	3.32±0.06	2.89±0.66[b]	3.64±0.17[c]	4.20±0.20[bc]	3.11±0.14	2.74±0.21	2.67±0.24[a]	2.97±0.30[a]
LVESD, mm	1.46±0.04	1.25±0.10	2.13±0.18[bc]	2.87±0.22[bc]	1.36±0.06	1.15±0.11	1.18±0.16[a]	1.41±0.24[a]
IVSTD, mm	0.66±0.02	1.26±0.05[b]	0.89±0.05[bc]	0.72±0.04[c]	0.86±0.06[a]	1.44±0.07[ab]	1.47±0.06[ab]	1.38±0.08[ab]
PWTD, mm	0.64±0.02	1.24±0.05[b]	0.91±0.05[bc]	0.72±0.03[c]	0.86±0.06[a]	1.45±0.07[ab]	1.48±0.06[ab]	1.44±0.08[ab]
RWT	0.39±0.01	0.88±0.05[b]	0.51±0.04[bc]	0.35±0.02[c]	0.57±0.06[a]	1.10±0.10[ab]	1.17±0.13[ab]	1.02±0.16[ab]
LVMi	2.59±0.17	5.20±0.41[b]	4.29±0.33[bc]	3.99±0.42 [b]	3.36±0.21[a]	6.35±0.78[b]	5.96±0.53[ab]	6.48±0.83[ab]
FS%	56.1±0.7	57.3±1.7	42.3±2.8[bc]	32.3±2.3[bc]	56.1±0.5	58.3±1.0	56.7±1.9[a]	54.0±3.6[a]

[a]$P<0.05$ vs WT.
[b]$P<0.05$ vs basal conditions.
[c]$P<0.05$ vs the previous examination.
BW indicates body wt, HR, heart rate, LVEDD, left ventricle end-diastolic diameter, LVESD, left ventricle end-systolic diameter, IVSTD, interventricular septum thickness in end-diastole, PWTD, posterior wall thickness in end-diastole, RWT, relative wall thickness, LVMi, left ventricular mass index, FS%, percent fractional shortening.

Melusin Overexpression Protects from Dilated Cardiomyopathy in Response to Long-Standing Pressure Overload

Mel-TG and WT mice were subjected to AB for 12 weeks, and serial echocardiography was performed to progressively monitor cardiac structure and function (Figure 3a).

Four weeks after banding, both mice strains showed increased interventricular septum, LV posterior wall thickness and LV mass index (Table 2). Concomitantly, LV end-diastolic diameter was decreased. Therefore, an increase in relative wall thickness was achieved in both mice groups (Table 2, Figure 3a,c). This remodeling represents a typical pattern of concentric hypertrophy, an adaptive compensatory mechanism to sustained hypertensive conditions. Although Mel-TG still showed a higher LV mass index, LVH response was similar in both mice groups (Δ % LVMI 92±23% versus 103±16%).

At 8 weeks of AB, WT mice showed reduction in LV wall thickness with a concomitant increase in LV end-diastolic

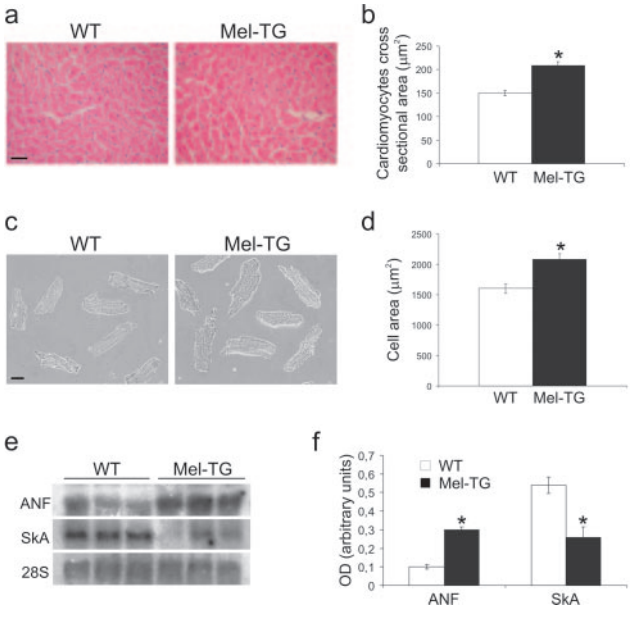

Figure 2. Melusin overexpression induces LV hypertrophy in basal condition. (a) Histological sections from WT and Mel-TG mice stained with hematoxylin-eosin. Scale bar:20 μm. (b) Cardiomyocyte cross-sectional area (30 sections from 3 mice per genotype). (c) Phase-contrast images of cardiomyocytes isolated from adult WT and Mel-TG hearts. Scale bar:20 μm. (d) Cell area (100 cardiomyocytes from 4 mice per genotype). (e) Northern blot for atrial natriuretic factor (ANF) and α-skeletal actin (SkA) on LV RNA. 28S rRNA as loading control. (f) Densitometric analysis on 6 mice per genotype normalized on 28S. (*): $P<0.05$ vs WT mice.

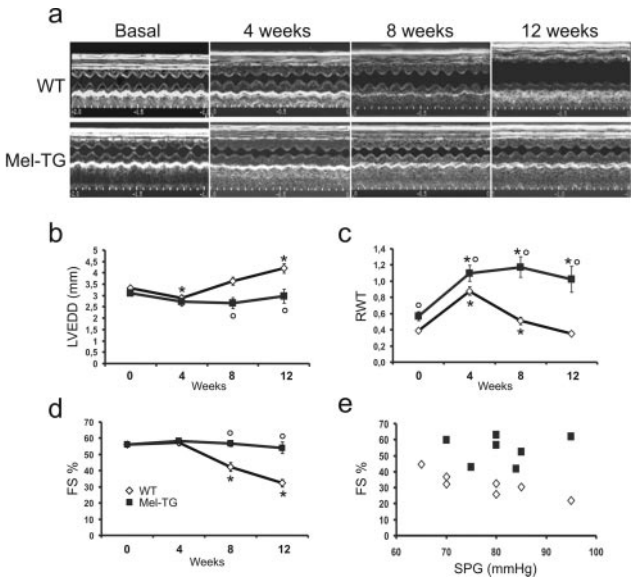

Figure 3. Melusin overexpression prevents LV dilation on prolonged pressure overload. (a) Representative M-mode LV echocardiographic recording of WT and Mel-TG in basal condition and after 4, 8, and 12 weeks of AB. Echocardiographic LV end diastolic diameter (LVEDD) (b), relative wall thickness (RWT) (c), and percent fractional shortening (FS%) (d). Relationship between systolic pressure gradient (SPG) and FS% in Mel-TG and WT mice after 12 weeks of AB (e). (*): $P<0.05$ vs basal conditions; (°):$P<0.05$ vs WT mice.

diameter (Table 2, Figure 3b) indicating an initial eccentric hypertrophic remodeling. Mel-TG mice, on the other hand, maintained values of LV wall thickness and diameters comparable to those developed after 4 weeks of AB. More importantly, systolic contractile function, as measured by fractional shortening (FS), was fully retained in Mel-TG, while significantly impaired in WT (Table 2, Figure 3d).

At 12 weeks of AB, WT mice showed a further dilation of the LV chamber combined with a greater thinning of the walls (Table 2, Figure 3a). These alterations were associated with a further reduction of contractile function, thus realizing the transition toward heart failure. In contrast, Mel-TG mice retained the LV concentric hypertrophy and systolic function detected at 8 weeks (Table 2, Figure 3). Hemodynamic evaluations indicated that, whereas WT mice showed a significantly reduced systolic function in terms of dP/dt max, Mel-TG preserved contractile function (Table 1). Moreover, maximum chamber elasticity (Emax) showed a significant increase in Mel-TG, but not in WT mice, further demonstrating a better contractile function in transgenic animals. Nevertheless, pressure overloaded LVs of both mice strains showed an impaired diastolic function, as detected by dP/dt min and τ Glantz.

SPG measured at 12 weeks of AB was similar in both study groups (Table 1). Finally, the relationship between SPG and FS revealed that Mel-TG mice show higher FS at any SPG studied, revealing the ability of melusin to protect against cardiac dysfunction in a wide range of pressure overload (Figure 3e).

All together these data indicate the ability of melusin overexpression to maintain concentric compensatory hypertrophic remodeling and to prevent the onset of heart failure.

Melusin Overexpression Induces Increased Phosphorylation of AKT/GSK3β and ERKs

Western blot analysis was performed to investigate the signaling events affected by melusin overexpression. Unstimulated LVs of Mel-TG mice showed increased Ser9 phosphorylation of GSK3β as compared with WT (Figure 4a,b). Mel-TG hearts also showed increased level of ERK1/2 phosphorylation after normalization on total ERK1/2 which were expressed at higher levels in Mel-TG mice.

We then tested the activation of these pathways in response to AB. After 10 minutes of AB, GSK3β was phosphorylated at a much higher level in Mel-TG compared with WT LV (Figure 4c,d). Similar differences were also observed for AKT, consistent with its role as a major kinase involved in Ser9 phosphorylation of GSK3β. ERK1/2 were also strongly phosphorylated in transgenic mice compared with WT. On the other hand, p38 phosphorylation in response to AB was not significantly different between the 2 mouse strains.

Increased phosphorylation of these signaling proteins in Mel-TG versus WT LVs persisted for the whole period of AB (Figure 4e,f). Increased phosphorylation of AKT in Mel-TG LVs at 12 weeks of AB was also detected by immunostaining of heart histological sections (not shown).

AKT and ERKs Signaling Mediate Melusin-Induced Cardiomyocyte Growth

In order to test if AKT and ERK have a causative role in melusin-induced cardiomyocyte hypertrophy, in vitro experiments were performed. To induce melusin overexpression, cultured rat embryo cardiomyocytes were infected with a lentiviral vector coding for melusin (Figure 5a). Consistent with in vivo experiments in transgenic hearts, melusin overexpressing cardiomyocytes underwent pronounced hypertrophy as assessed by surface area measurements (Figure 5b,c). This response was strongly blunted by treatment either with PD98059, a MEK-1 inhibitor that prevented ERK1/2 phosphorylation (85% inhibition), or with a phosphatidylinositol analog inhibiting AKT (73% inhibition). These data indicate that, AKT and ERK play a crucial role in the hypertrophy response induced by melusin overexpression.

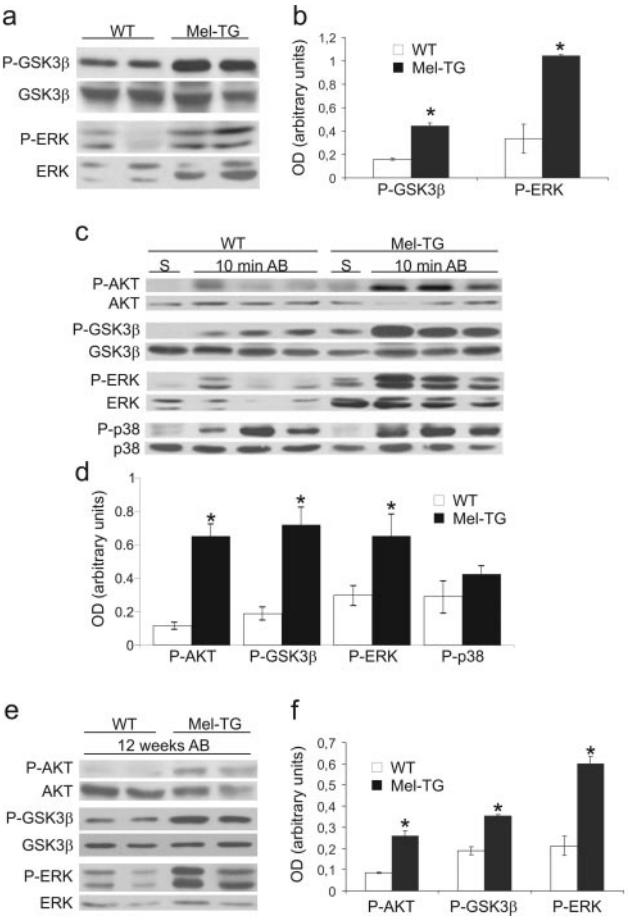

Figure 4. Melusin overexpression enhances phosphorylation of AKT, GSK3β, and ERK1/2. Representative western blot of WT and Mel-TG mice performed using antibodies to the indicated signaling molecules and their phosphorylated (P-) forms (a,c,e). Densitometric mean values of the phosphorylated species normalized to the expression level of the corresponding proteins (n=7 per genotype) (b,d,f). LV in basal conditions (a,b), of sham-operated mice (S) and mice subjected to 10 minutes (c,d) or 12 weeks of AB (e,f). (*): $P<0.05$ vs WT.

Melusin Overexpression Protects From Apoptosis and Fibrosis Induced by Long-Standing Pressure Overload

As AKT, GSK3β, and ERK signaling can protect from apoptosis, we measured apoptotic index in hearts subjected to 12 weeks of pressure overload. WT LVs showed a high number of TUNEL-positive cells (Figure 6a,b), consistent

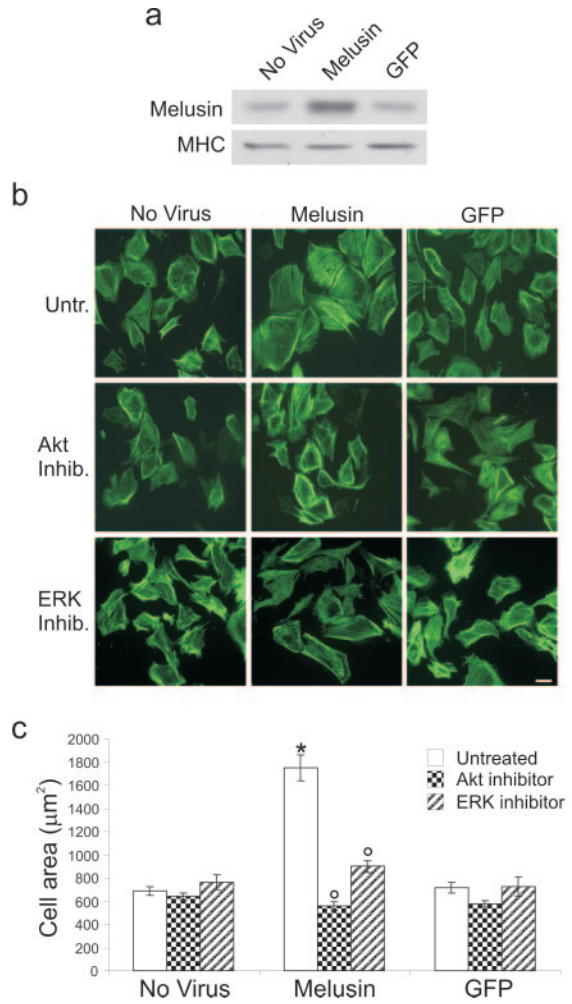

Figure 5. AKT and ERK signaling are required for melusin-induced cardiomyocyte growth. Rat embryo cardiomyocytes were infected with a lentiviral vector coding for melusin or GFP as control. Melusin expression detected by western blot analysis (a). Cardiomyocytes hypertrophy as assessed by surface area measurements (b,c). Melusin-induced hypertrophy was strongly blunted by treatment for 72 hours with either 50 μmol/L PD98059, an ERK1/2 inhibitor, or 20 μmol/L phosphatidylinositol analog inhibiting AKT phosphorylation (b,c). Cell areas were calculated on 70 cardiomyocytes for each group in 3 independent experiments. (*): $P<0.01$ versus no virus, (°): $P<0.01$ vs melusin untreated. Scale bar: 20 μm.

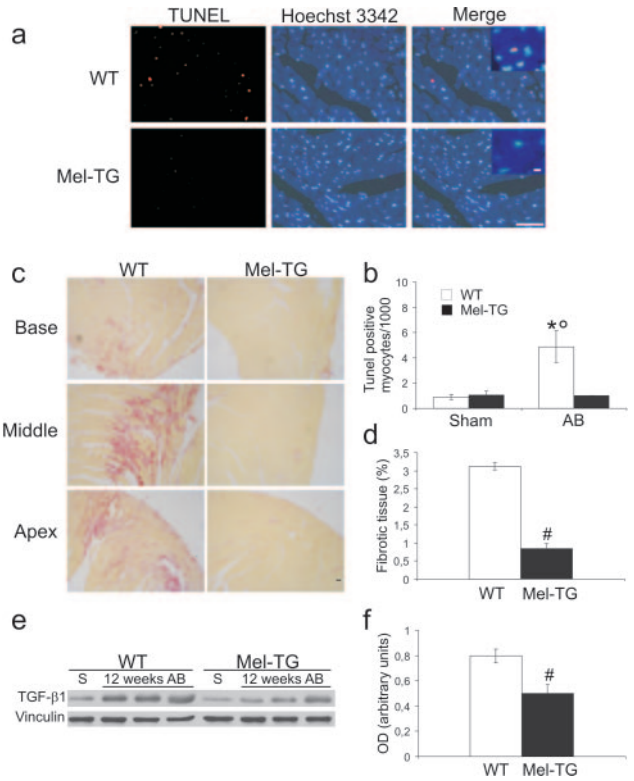

Figure 6. Melusin overexpression protects from cardiomyocyte apoptosis and prevents fibrotic tissue deposition induced by pressure overload. (a) TUNEL staining (red) on histological sections from WT and Mel-TG hearts subjected to 12 weeks of AB. Nuclei were counterstained with Hoechst-3342 (blue). Scale bars:100 μm and 10 μm (insets). (b) TUNEL-positive cardiomyocytes were quantified by counting only nuclei within myocytes. 30 histological sections from 3 different hearts per genotype. (c) Picrosirius red staining on histological sections from WT and Mel-TG LV after 12 weeks of AB. Scale bar:100 μm. (d) Fibrotic area quantified by image-analyzing system on histological sections from 3 different hearts per genotype (10 sections/mouse) and expressed as percentage of LV wall area. (e) Western blot analysis of TGF-β1 from WT and Mel-TG LV after sham operation (S) and 12 weeks of AB. Vinculin was used as sample loading control. Three representative mice per genotype are shown. (f) Mean values of TGF-β 1 expression from 7 banded hearts per genotype obtained by densitometric analysis. (*): $P<0.05$ vs sham; (°): $P<0.05$ versus Mel-TG after AB. (#): $P<0.05$ vs WT.

with previous reports indicating that apoptosis is a major event involved in the onset of heart failure on prolonged pressure overload.[10] In contrast, Mel-TG LV subjected to 12 weeks of pressure overload showed a number of TUNEL-positive cardiomyocytes not significantly different from that of sham-operated mice.

Heart sections were also stained with Picrosirius red to detect fibrosis. Deposition of stromal connective tissue was strongly reduced in melusin transgenic LV after 12 weeks of pressure overload compared with WTs (Figure 6c and 6d). Western blot analysis further indicated that after AB levels of TGF-β1, a major pro-fibrotic cytokine, were 47% lower in Mel-TG LV (Figure 6e and 6f).

After 12 weeks of pressure overload, capillary density, a parameter that participates in heart remodeling, was 26.3% higher in Mel-TG LV compared with WT ($P<0.05$).

Melusin Overexpression Regulates Genes Involved in Fibrosis and Inflammation

Global transcriptome analysis in WT and Mel-TG LV subjected to AB for 12 weeks was performed using an oligonucleotide array representing ≈13 000 mouse genes. LV samples from 2 different Mel-TG mice were compared in competitive hybridization to WT, and experiments were repeated twice. Comparison of the expression profile revealed 110 differentially expressed genes, 68 underexpressed and 42 overexpressed in Mel-TG hearts compared with WT. The complete dataset is reported at http://muscle.cribi.unipd.it/microarrays/melusin/. Genes coding for extracellular matrix proteins, leukocyte markers, and cytokines were the largest functionally related gene clusters differentially expressed in the 2 mice strains. This strongly indicates that fibrosis and inflammation are significantly depressed in Mel-TG versus WT LVs subjected to chronic pressure overload (Online

Table 1). Interestingly, kallikrein, a protease capable of releasing kinins and inducing collagen breakdown, was upregulated in Mel-TG consistently with its role as an antifibrotic gene.[11,12] Moreover, SkA was greatly reduced in Mel-TG versus WT banded hearts, thus confirming that reduced expression of SkA is characteristically retained during the 12 weeks of hypertrophic remodeling.

Discussion

Here we report that overexpression of melusin, a recently described integrin-binding protein,[3] in hearts of transgenic mice, induceds a modest, but significant, level of LVH in basal condition. Moreover, in response to chronic pressure overload, melusin overexpression allows sustained compensatory LVH and prevents the transition toward heart failure. Because loss of melusin causes reduced LVH followed by heart dilation and failure in response to hemodynamic overload,[4] we conclude that melusin is an important molecule controlling beneficial remodeling of LV.

The protection against heart failure observed in Mel-TG subjected to aortic constriction could be influenced, at least initially, by the presence of a basal LVH leading to reduced wall stress. Recent experimental evidence, however, indicate that normalization of wall stress is not crucial to prevent the evolution toward cardiac dysfunction in response to pressure overload. In fact, mice defective for Gq signaling and for norepinephrine synthesis do not develop heart failure despite markedly blunted cardiac growth response to pressure overload and abnormally higher wall stress.[13] Thus, normalization of wall stress is not the main variable in the evolution of overloaded hearts toward heart failure, but other factors such as the quality of cardiac hypertrophy can play a crucial role.

LV adaptive hypertrophy induced by melusin overexpression showed specific molecular features. In particular, analysis of LVH markers indicated that SkA, a prominent fetal actin isoform, is downregulated in Mel-TG heart versus WT both in basal conditions and after 12 weeks of AB. Consistent with the hypothesis of melusin acting as a stretch sensor downstream integrin signaling, SkA gene promoter is silenced in cultured fibroblast stretched by mechanical force applied to β1 integrin with collagen-coated magnetic beads.[14] In contrast, SkA is upregulated in experimental mouse models of chronic pressure overload and in human heart failure,[15] but downregulated or unchanged in exercise-induced cardiac hypertrophy.[16] The finding that SkA was downregulated in Mel-TG versus WT LV suggests that, in conditions of pressure overload, cardiac hypertrophy in Mel-TG partially mimics that observed in exercise-induced cardiac hypertrophy.

An additional feature of LVH of Mel-TG mice is absence of fibrosis as detected by both histological analysis and gene profiling experiments. This could be ascribed to negative regulation of well-known profibrotic factors such as TGF-β 1, and to upregulation of antifibrotic factors such as kallikrein. In this respect it is worth noting that forced expression of kallikrein gene in heart of diabetic rats prevents fibrosis and ameliorates ventricle function.[14] Accumulation of stromal tissue represents a deleterious feature of LVH affecting the viscoelastic properties of the myocardium, impairing diastolic function and favoring the transition toward heart failure. The reduced fibrosis in Mel-TG overloaded LV could lead to improvement of diastolic function. This, however, was not the case since impairment of LV diastolic function was comparable in Mel-TG and WT mice in conditions of pressure overload. Indeed, fibrosis is only one of several determinants of diastolic function,[17] and hypertensive conditions represent another crucial factor, evoking an impairment of LV diastolic function independently of their impact on cardiac hypertrophic remodeling.[18] Thus, the hypertensive conditions imposed by AB in both Mel-TG and WT mice may mask the impact on diastolic function of reduced fibrosis.

Finally, additional important features of AB-induced heart remodeling in Mel-TG mice are reduced inflammatory reaction and increased capillary density, two additional features of the exercise-induced hypertrophy.[19]

Previous findings have shown that melusin ablation impairs phosphorylation of AKT and GSK3β[4] in response to pressure overload. Here we show that, in basal conditions, Mel-TG hearts display higher GSK3β and ERK1/2 phosphorylation. Moreover, these phosphorylations are further increased in Mel-TG LV after pressure overload and maintain a higher level over WT after 12 weeks of AB. Interestingly, inhibitors of AKT and ERK1/2 block melusin-induced hypertrophy in cultured rat embryo cardiomyocytes. These data, although obtained in a cell culture model with growth features different from those of adult cardiomyocytes, support a causative role for AKT and ERK1/2 in melusin-induced LVH. The mechanisms by which melusin controls AKT phosphorylation are unknown at present. Several examples of adaptor proteins devoid of enzymatic activity, such as Shc and Grb2, and p130Cas are known to regulate different kinases. The most likely hypothesis is that melusin can function as an adaptor molecule interacting with proteins regulating AKT activation. AKT controls phosphorylation of mTor, p70S6K and GSK3β, three serine/threonine kinases responsible for increased protein synthesis. Forced expression of constitutively active AKT in the heart of transgenic mice induces increased cardiomyocyte size and concentric hypertrophy in the absence of fibrosis with preserved systolic function.[20] In addition expression of a nonphosphorylable form of GSK3β prevents LVH in response to pressure overload as well as other hypertrophic stimuli.[21] In agreement with these findings, lack of GSK3β phosphorylation in response to pressure overload is associated with reduced LVH and development of dilated cardiomyopathy,[4,22] pointing to an important role of melusin-induced AKT and GSK3β overphosphorylation to sustain an adaptive concentric LVH.

A number of studies implicate ERK1/2 signaling as an important regulator of LVH.[23] In particular, overexpression of MEK1, an upstream activator of ERK1/2, in transgenic mice leads to development of compensatory LVH.[24] The increased ERK1/2 phosphorylation observed in Mel-TG heart, both in basal condition and after AB is, thus, in line with the compensated hypertrophy phenotype observed in our transgenic mice.

AKT, GSK3β, and ERK1/2 are among the main signaling proteins involved in the anti apoptotic machinery.[25] AKT inhibits caspase 9 and the proapoptotic molecule Bad, stimulates the prosurvival factor Bcl-2, and phosphorylates fork-

head transcription factors, repressing their ability to promote proapoptotic genes. In addition, transgenic mice overexpressing MEK1 in the heart show reduced cardiomyocyte apoptosis in a model of ischemia-reperfusion injury.[26] GSK3β is also involved in protecting cardiomyocytes against apoptosis by regulating the mitochondrial permeability transition pore complex, which plays a central role in mitochondria-mediated cell death.[27] Involvement of these signaling molecules downstream melusin can, thus, explain the protection from apoptosis observed in transgenic hearts subjected to pressure overload.

In conclusion these data indicate that melusin overexpression allows sustained concentric compensatory cardiac hypertrophy in response to chronic pressure overload. LV remodeling in Mel-TG mice displays several features observed in hearts undergoing hypertrophy in response to physical training such as reduced fibrosis, apoptosis and inflammation and increased capillary density. This is likely to occur through the regulation of protective pathways maintaining a proportional balance between cardiac muscle and stromal tissue in overloaded LV. Because melusin expression increases in compensated hypertrophic LV subjected to pressure overload, but returns to basal level in dilated heart, upregulation of melusin expression could represent a novel strategy to activate beneficial signaling in LV remodeling and prevent the transition toward heart failure in response to hemodynamic overload.

Acknowledgments

This work was supported by grants from: Telethon to GT; Ministry of University and Research (FIRB, and PRIN) to GT and GL; Ministry of Health to GL. We wish to thank Ornella Azzolino, Immacolata Carfora and Giovanni Russo for technical assistance; Daniela Bongioanni, for helping in some experiments; Luigi Naldini and Elisa Vigna for providing lentiviral vectors and helping in virus production.

References

1. Hunter JJ, Chien KR. Signaling pathways for cardiac hypertrophy and failure. *N Engl J Med*. 1999;341:1276–1283.
2. Frey N, Olson EN. Cardiac hypertrophy: the good, the bad, and the ugly. *Annu Rev Physiol*. 2003;65:45–79.
3. Brancaccio M, Guazzone S, Menini N, Sibona E, Hirsch E, De Andrea M, Rocchi M, Altruda F, Tarone G, Silengo L. Melusin is a new muscle-specific interactor for beta(1) integrin cytoplasmic domain. *J Biol Chem*. 1999;274:29282–29288.
4. Brancaccio M, Fratta L, Notte A, Hirsch E, Poulet R, Guazzone S, De Acetis M, Vecchione C, Marino G, Altruda F, Silengo L, Tarone G, Lembo G. Melusin, a muscle-specific integrin beta1-interacting protein, is required to prevent cardiac failure in response to chronic pressure overload. *Nat Med*. 2003;9:68–75.
5. Gulick J, Subramaniam A, Neumann J, Robbins J. Isolation and characterization of the mouse cardiac myosin heavy chain genes. *J Biol Chem*. 1991;266:9180–9185.
6. Vecchione C, Fratta L, Rizzoni D, Notte A, Poulet R, Porteri E, Frati G, Guelfi D, Trimarco V, Mulvany MJ, Agabiti-Rosei E, Trimarco B, Cotecchia S, Lembo G. Cardiovascular influences of alpha1b-adrenergic receptor defect in mice. *Circulation*. 2002;105:1700–1707.
7. Wolska BM, Solaro RJ. Method for isolation of adult mouse cardiac myocytes for studies of contraction and microfluorimetry. *Am J Physiol*. 1996;271:H1250—H1255.
8. Kaddoura S, Firth JD, Boheler KR, Sugden PH, Poole-Wilson PA. Endothelin-1 is involved in norepinephrine-induced ventricular hypertrophy in vivo. Acute effects of bosentan, an orally active, mixed endothelin ETA and ETB receptor antagonist. *Circulation*. 1996;93:2068–2079.
9. Bonci D, Cittadini A, Latronico MV, Borello U, Aycock JK, Drusco A, Innocenzi A, Follenzi A, Lavitrano M, Monti MG, Ross J Jr, Naldini L, Peschle C, Cossu G, Condorelli G. 'Advanced' generation lentiviruses as efficient vectors for cardiomyocyte gene transduction in vitro and in vivo. *Gene Ther*. 2003;10:630–636.
10. Condorelli G, Morisco C, Stassi G, Notte A, Farina F, Sgaramella G, de Rienzo A, Roncarati R, Trimarco B, Lembo G. Increased cardiomyocyte apoptosis and changes in proapoptotic and antiapoptotic genes bax and bcl-2 during left ventricular adaptations to chronic pressure overload in the rat. *Circulation*. 1999;99:3071–3078.
11. Tschope C, Walther T, Koniger J, Spillmann F, Westermann D, Escher F, Pauschinger M, Pesquero JB, Bader M, Schultheiss HP, Noutsias M. Prevention of cardiac fibrosis and left ventricular dysfunction in diabetic cardiomyopathy in rats by transgenic expression of the human tissue kallikrein gene. *Faseb J*. 2004;18:828–835.
12. Gallagher AM, Yu H, Printz MP. Bradykinin-induced reductions in collagen gene expression involve prostacyclin. *Hypertension*. 1998;32:84–88.
13. Esposito G, Rapacciuolo A, Naga Prasad SV, Takaoka H, Thomas SA, Koch WJ, Rockman HA. Genetic alterations that inhibit in vivo pressure-overload hypertrophy prevent cardiac dysfunction despite increased wall stress. *Circulation*. 2002;105:85–92.
14. Lew AM, Glogauer M, McUlloch CA. Specific inhibition of skeletal alpha-actin gene transcription by applied mechanical forces through integrins and actin. *Biochem J*. 1999;341(Pt 3):647–653.
15. Haase D, Lehmann MH, Korner MM, Korfer R, Sigusch HH, Figulla HR. Identification and validation of selective upregulation of ventricular myosin light chain type 2 mRNA in idiopathic dilated cardiomyopathy. *Eur J Heart Fail*. 2002;4:23–31.
16. Diffee GM, Seversen EA, Stein TD, Johnson JA. Microarray expression analysis of effects of exercise training: increase in atrial MLC-1 in rat ventricles. *Am J Physiol Heart Circ Physiol*. 2003;284:H830—H837.
17. Zile MR, Brutsaert DL. New concepts in diastolic dysfunction and diastolic heart failure: Part II: causal mechanisms and treatment. *Circulation*. 2002;105:1503–1508.
18. Gelpi RJ, Pasipoularides A, Lader AS, Patrick TA, Chase N, Hittinger L, Shannon RP, Bishop SP, Vatner SF. Changes in diastolic cardiac function in developing and stable perinephritic hypertension in conscious dogs. *Circ Res*. 1991;68:555–567.
19. Brodal P, Ingjer F, Hermansen L. Capillary supply of skeletal muscle fibers in untrained and endurance-trained men. *Am J Physiol*. 1977;232:H705–H712.
20. Condorelli G, Drusco A, Stassi G, Bellacosa A, Roncarati R, Iaccarino G, Russo MA, Gu Y, Dalton N, Chung C, Latronico MV, Napoli C, Sadoshima J, Croce CM, Ross J Jr. Akt induces enhanced myocardial contractility and cell size in vivo in transgenic mice. *Proc Natl Acad Sci U S A*. 2002;99:12333–12338.
21. Antos CL, McKinsey TA, Frey N, Kutschke W, McAnally J, Shelton JM, Richardson JA, Hill JA, Olson EN. Activated glycogen synthase-3 beta suppresses cardiac hypertrophy in vivo. *Proc Natl Acad Sci U S A*. 2002;99:907–912.
22. Badorff C, Ruetten H, Mueller S, Stahmer M, Gehring D, Jung F, Ihling C, Zeiher AM, Dimmeler S. Fas receptor signaling inhibits glycogen synthase kinase 3 beta and induces cardiac hypertrophy following pressure overload. *J Clin Invest*. 2002;109:373–381.
23. Bueno OF, Molkentin JD. Involvement of extracellular signal-regulated kinases 1/2 in cardiac hypertrophy and cell death. *Circ Res*. 2002;91:776–781.
24. Bueno OF, De Windt LJ, Tymitz KM, Witt SA, Kimball TR, Klevitsky R, Hewett TE, Jones SP, Lefer DJ, Peng CF, Kitsis RN, Molkentin JD. The MEK1-ERK1/2 signaling pathway promotes compensated cardiac hypertrophy in transgenic mice. *Embo J*. 2000;19:6341–6350.
25. Datta SR, Brunet A, Greenberg ME. Cellular survival: a play in three Akts. *Genes Dev*. 1999;13:2905–2927.
26. Lips DJ, Bueno OF, Wilkins BJ, Purcell NH, Kaiser RA, Lorenz JN, Voisin L, Saba-El-Leil MK, Meloche S, Pouyssegur J, Pages G, De Windt LJ, Doevendans PA, Molkentin JD. MEK1-ERK2 signaling pathway protects myocardium from ischemic injury in vivo. *Circulation*. 2004;109:1938–1941.
27. Juhaszova M, Zorov DB, Kim SH, Pepe S, Fu Q, Fishbein KW, Ziman BD, Wang S, Ytrehus K, Antos CL, Olson EN, Sollott SJ. Glycogen synthase kinase-3beta mediates convergence of protection signaling to inhibit the mitochondrial permeability transition pore. *J Clin Invest*. 2004;113:1535–1549.

Material and Methods

Generation of transgenic mice

The SalI-BamHI alpha-MHC promoter DNA fragment, obtained from J. Robbins[1], was cloned into SalI-ApaI digested pBluescriptII vector construct containing the myc-tagged cDNA of human melusin followed by β-globin intron and poly-A (Figure 2a). The construct was microinjected in fertilized eggs of FVB mice and transgenic integration was confirmed by southern blot analysis of KpnI digested DNA (Figure 2b) and by PCR analysis, using the following primers: forward CGATATGGAGCAGAAGCTGATC, reverse GATCAGACTGTCAAGTCCTG. The use of animals was in compliance with the guidelines of the European Community and was approved by the Animal Care and Use Committee of the University of Torino.

Transthoracic Echocardiography

Transthoracic echocardiographic analysis was performed in conscious mice using a General Electric System Five Performance cardiac ultrasound machine, equipped with a 10 MHz imaging transducer. Using the 2D parasternal short-axis imaging as a guide, a left ventricular M-mode tracing was obtained in conscious mice. End-diastolic and systolic interventricular septum (IVSTd, IVSTs), posterior wall thickness (PWTd, PWTs) and left ventricular internal diameters (LVEDD, LVESD) were measured using a computed NIH image analysis system. Percent fractional shortening (%FS) and relative wall thickness (RWT) were calculated according to the following standard formulas:

$$\%FS = [(LVEDD-LVESD)/LVEDD] \times 100$$

$$RWT = [(IVSd+PWd)/2]/(LVEDD/2)$$

Reproducibility, calculated as the difference between two determinations divided by the mean of the two determinations and expressed as percentage of error, was 3.5±.5 for LV diameters and 6.9±.8 for wall thickness. Serial echocardiographic evaluations were assessed in mice in basal conditions and during chronic pressure overload (4-8-12 weeks after banding).

Left ventricular haemodynamic

Mice were anesthetized as described[2] with an intraperitoneal injection of tribromoethanol (Avertin, 350 mg/kg) and inotropic and lusitropic function were evaluated by measuring intraventricular volume and pressure with a micromanometer catheter (Millar 1.4 F, SPR 671, Millar Instruments, Inc., USA) positioned in the left ventricle via right common carotid artery canulation[3]. The maximum rate of left ventricular pressure developed (dP/dt max) expressed systolic function, while left ventricular pressure decay (dP/dt min) and time constant of relaxation (τ Glantz) identified diastolic function. The haemodynamic analysis was performed in aortic banded and sham-operated animals after 12 weeks from surgical procedures.

Left ventricular pressure overload

A chronic pressure overload was imposed to the left ventricle through transverse aortic banding (AB) between *truncus anonimus* and left carotid artery, as previously described[3]. To evaluate the degree of pressure overload imposed on the left ventricle, systolic pressure gradient (SPG) was measured by selective cannulation of left and right carotid arteries during the haemodynamic analysis at 12 weeks of aortic banding[4]. A further group underwent the same surgical procedures without aortic stenosis (Sham). After haemodynamic evaluations, the mice were weighted, then the hearts were excised and processed for further molecular analysis.

Conscious blood pressure measurement

Conscious blood pressure and heart rate were measured in unrestrained conditions by a radiotelemetric device (TA11PA-C20, Data Sciences International, St. Paul, MN, USA) whose sensing catheter was inserted into the femoral artery, as previously described[2]. After implantation

mice were housed in a single cage and allowed 10 days recovery from surgical procedures. Blood pressure and heart rate were continuously recorded for 4 hours (from 8:00AM to 12:00AM) for 4 consecutive days. Telemetered pressure signals were stored and analyzed by a dedicated computed data acquisition system (Dataquest Acquisition and Analysis System, DQ ART 1.1 Gold, Data Sciences International, St. Paul, MN, USA) that calculated the mean value during the acquisition time.

Histological analysis

For histological analysis, hearts were fixed with PFA 4% in 20 mM phosphate buffer pH 7,5 overnight at 4°C and paraffin embedded. 5 μm sections were cut at the frontal axis plane. Histological section were stained with hematoxylin/eosin for standard analysis and with Picrosirious red to stain collagen fibers. To quantify fibrosis, whole ventricle slice picture were taken using a 12x stereoscopic microscope and analysis of fibrotic area were performed using ImageProPlus software. Areas of fibrosis were calculated as percentage of total area of the left ventricle. Apoptotic cells were detected by the TUNEL reaction on paraffin embedded heart sections using the TMR red kit (Roche) with no pre-incubation with proteinase K. Nuclei were also counterstained with Hoechst 3342 1μg/ml for 5 min at room temperature. To measure myocyte area and capillary density, suitable cross sections were defined as having nearly circular capillary profiles and nuclei. Capillaries were identified by anti von Willebrand factor antibodies (Sigma) followed by peroxidase labeled secondary antibodies as described[5]. For all quantitative analysis mentioned above, 3 mice for each genotype and 10 histological sections from each heart were analyzed.

Isolation of Adult Cardiac Myocytes and Morphometric Analysis

Cardiac myocytes were enzymatically dissociated from hearts of wild type and melusin over-expressing mice as previously described[6]. Briefly, heart was removed and the aorta was cannulated on a perfusion system. Retrograde perfusion of calcium-free buffer was used to arrest the heart. Heart was, then, perfused with a collagenase-based solution to dissociate myocytes that were plated on laminin-coated substrate after gradual reintroduction of calcium in the presence of 10 mM 2,3-Butanedione Monoxime to inhibit contractility. Two hours after plating, cardiomyocytes were photographed at 20x phase contrast using an inverted microscope and cell areas were measured using ImageProPlus software. Total 100 cardiomyocytes per mouse genotype from four independent experiments were measured.

Northern blot analysis

10 μg of total RNA extracted from left ventricles with the Trizol reagent (Invitrogen) were separated by electrophoresis in 1,5% denaturing formaldehyde agarose-gels and blotted to Hybond nylon membranes (Amersham Biosciences). Membranes were probed with atrial natriuretic factor (ANF) and alpha-skeletal actin (SkA) radiolabeled probes. Band intensities were determined by densitometric analysis from two independent experiments with a total of 6 mice for each genotype.

Embryonic cardiomyocyte isolation and transduction

Ventricular cardiomyocytes were prepared from E19 old Sprague-Dawley rat hearts by enzyme digestion as described[7]. Ventricles were separated from atria and excess vessels and rinsed in 1x ADS solution (116mM NaCl, 20mM HEPES, 0.8mM NaH_2PO_4, 5,4mM KCl, 0,8mM $MgSO_4$, 55mM glucose). Ventricles were cut into four pieces and subjected to a series of digestions with collagenase (type 2, Worthington Biochemical Corporation, Lakewood, NJ) and pancreatin (Sigma) at a concentration of 80.6 units/ml and 62.5 μg/ml, respectively, in 1x ADS solution. Cells were than resuspended in plating medium (4 parts DME and 1 part M199, 10% horse serum, 5% new born calf serum, 100 U/ml penicillin/streptomycin) and seeded in a petri at 37°C for 60 minutes to allow fibroblast adhesion. Non adherent cells were collected and plated onto laminin coated dishes

at the density of $2.5x10^4$ cells in 24-well plates. The final myocyte cultures contained >95% cardiomyocytes as determined by actin staining. After 24 h, medium was changed to maintenance medium (4 parts DME an 1 part M199, 5% horse serum, 0.5% new born calf serum, 100 U/ml penicillin/streptomycin) for the duration of the experiment.
In order to express melusin in these cells, lentiviral vector coding for myc tagged human melusin, and a control vector coding for GFP, were prepared as described[8]. As transfer vector plasmids we used pRRLcPPT.hPGK.MYC-MEL.WPRE and pRRLcPPT.hPGK.GFP.WPRE. These plasmids contains respectively the myc-tagged human melusin gene and the enhanced GFP marker gene driven by the human phosphoglycerate kinase promoter (hPGK). Viral stocks were prepared at 10^6 TU/ml, corresponding to 100 ng p24/ml.
48 h after cardiomyocyte plating, medium was removed and replaced with 1 ml supernatant containing lentiviral vector (100 ng p24) to which 8 μg/ml of Polybrene had been added. Cells were kept overnight at 37°C, washed twice with cold PBS and incubated for 72 h in fresh medium with or without inhibitors indicated below. Infection efficiency was approximately 80% as assessed by GFP fluorescence. To inhibit ERK1/2 and AKT, cells were incubated for 72 h with 50μM MEK-1 inhibitor (PD98059, Calbiochem) or 20μM AKT inhibitor (1L-6-hydroxymethyl-chiro-inositol 2(R)-2-O-methyl-3-O-octadecylcarbonate, Calbiochem). Under these conditions ERK1/2 phosphorylation was inhibited by 85%, while AKT phosphorylation was inhibited by 73% as indicated by western blot analysis with phospho specific antibodies. At the end of the incubation time cells were either fixed and stained with FITC–labeled phalloidin (Sigma) or subjected to western blot analysis as described below.

Western blot analysis

Left ventricles were rapidly dissected, washed in cold PBS and frozen in liquid nitrogen, homogenized with a pestle. Powders were resuspended in 1% Triton X-100, 150mM NaCl, 50mM Tris-HCl pH 8, 1 mM Na_3VO_4, 10 mM NaF, 10 μg/ml leupeptin, 4 μg/ml pepstatin, 0,1 TIU/ml aprotinin), incubated for 1 h at 4°C and centrifuged at 14000 RPM at 4°C to remove debris. Protein concentration was quantified using Biorad and 50 μg samples were separated by SDS-PAGE followed by western blotting. Blots were probed with the following antibodies: antibodies to phospho-Ser9-GSK3β, to phospho-Ser473-AKT, to AKT and to phospho-ERK1/2 were from New England BioLabs; to GSK3β, to ERK1 (C16) and to TGF-β1 were from Santa Cruz Biotechnology; to p38, and to phospho-p38 were from Calbiochem, to Myc epitope and to vinculin from Sigma. The MF-20 monoclonal antibody to myosin heavy chain was obtained from the Developmental Studies Hybridoma Bank. Polyclonal antibodies to melusin were prepared as previously described[9].

Transcriptome analysis

Microarray fabrication: the mouse microarray platform was made with a collection of 13,443 70mer oligonucleotides (Qiagen-Operon, version 1.1). Each oligonucleotide was spotted in two replicates on MICROMAX SuperChip I glass slides (Perkin-Elmer) using Biorobotics Microgrid II (Apogent Discoveries), supplied with 48 stealth micro pins.
RNA purification and labeling: frozen left ventricles were homogenized for 3–5 min using an ultra-turrax-T8 blender (IKA-Werke) in 5 volumes of TRIZOL reagent (Invitrogen/Life Technologies). Total RNA was purified using RNeasy Mini Kit (Qiagen). RNA was subjected to quality control using Agilent Bioanalyzer 2100 (Agilent Technologies). Linear amplification of mRNA from 500ng of total RNA was carried on using the Amino Allyl Message-Amp-aRNA kit (Ambion) with one round of amplification according to the manufacturer's recommendations. 7μg of aRNA from each sample was coupled to Cy3 or Cy5 dyes (Amersham Pharmacia Biotech) to obtain labeled aRNA ready for microarray hybridization.
Microarray hybridization: Labeled RNAs were concentrated by ethanol precipitation and dissolved in 115μl of hybridization buffer (5XSSC, 0.1% SDS, 25% formamide). Labeled aRNA target from wild type and Mel TG heart samples were mixed before precipitation. After denaturation at 90°C

for 2 min, the labeled targets were added to the microarrays, previously incubated in pre-hybridization buffer (5X SSC, 0.1% SDS,100ng/ul ss-DNA, 5X Denhardt) for 2-3 hours at 48°C. Hybridization was carried on overnight at 48°C in an ArrayBooster microarray incubator (Advalytix), followed by a series of post-hybridization washings. Competitive hybridization was done twice using different microarray slides in which each single sample and control RNA was labeled either with Cy3 or Cy5 fluorochromes (dye-swapping procedure). Using this strategy, we obtained four fluorescence intensity values for each probe in the platform. After spot normalization (see below), the average value of probe replicates was calculated. Fluorescence detection was carried out on a GSI Lumonics LITE dual confocal laser scanner (Perkin-Elmer) with ScanArray Microarray Analysis Software, and raw scanner images were analyzed with QuantArray software (Perkin-Elmer). Normalization of the expression levels was performed with MIDAS program (TIGR Microarray Data Analysis System, http://www.tigr.org/software/tm4/). We then performed global and Lowess mean normalizations across element signal intensity and then logarithmic transformation was applied at each expression ratio.

Detection of differentially expressed transcripts: the $\log_2$ expression ratios calculated by MIDAS on each array probe of each competitive hybridization experiment were processed for consistency by the Statistical Analysis of Microarrays software (SAM, http://www-stat.stanford.edu/tibs/SAM/index.html). SAM is a non-parametric statistical test based on a permutation approach specifically implemented for microarray data. On the basis of the SAM output, we chose as threshold level for False Discovery Rate 0.74%. With this value we obtained 110 differentially expressed genes (68 under-expressed and 42 over-expressed in Mel TG versus wild type mice).

Online Table 1. Gene expression profiling of Mel-TG hearts subjected to 12 weeks of AB.

GENE DESCRIPTION	GENE SYMBOL	GenBank ID	EXPRESSION CHANGES
ACTIN, ALPHA, SKELETAL MUSCLE 1	Acta1	M12347	**-2.7**
FIBROSIS			
COLLAGEN, TYPE III, ALPHA 1	COL3A1	X52046	**-2.8**
COLLAGEN, TYPE XV	COL15A1	AF011450	**-2.2**
COLLAGEN, TYPE XIV, ALPHA 1	COL14A1	AJ131395	**-2.2**
COLLAGEN, TYPE VI, ALPHA 3	COL6A3	AF064749	**-1.6**
COLLAGEN, TYPE VI, ALPHA 1	COL6A1	X66405	**-1.9**
COLLAGEN, TYPE I, ALPHA 1	COL1A1	U08020	**-1.6**
COLLAGEN, TYPE V, ALPHA 2	COL5A2	L02918	**-1.9**
PROCOLLAGEN C-ENDOPEPTIDASE ENHANCER 2	PCOLCE2	AK010249	**-1.5**
FIBRILLIN 1	FBN1	L29454	**-1.6**
LUMICAN	LUM	AF013262	**-1.7**
BIGLYCAN	BGN	L20276	**-2.1**
FIBROMODULIN	FMOD	X94998	**-1.4**
SECRETED MODULAR CALCIUM-BINDING PROTEIN 2	SMOC2	NM_022315	**-1.9**
KALLIKREIN 26	Klk26	NM_010644	**+0.7**
LEUKOCYTES/INFLAMATION			
HISTOCOMPATIBILITY 2, CLASS II ANTIGEN A, ALPHA	H2-Aa	NM_010378	**-2.6**
HISTOCOMPATIBILITY 2, O REGION BETA LOCUS	H2-Ob	AF027865	**-2.4**
THYMIC STROMAL-DERIVED LYMPHOPOIETIN, RECEPTOR	Tslpr	AF201963	**-1.7**
IA-ASSOCIATED INVARIANT CHAIN	Ii	X05430	**-1.9**
INTERFERON GAMMA RECEPTOR	Ifngr1	M28233	**-1.5**
CHEMOKINE (C-C MOTIF) LIGAND 21B (SERINE)	Ccl21b	AF001980	**-1.5**
CD14 ANTIGEN	Cd14	M34510	**-1.4**
LYSOZYME	Lyzs	NM_017372	**-1.5**
COMPLEMENT COMPONENT 1, R SUBCOMPONENT	C1r	NM_023143	**-1.4**
CHEMOKINE (C-C MOTIF) LIGAND 21A (LEUCINE)	Ccl21a	U88322	**-1.5**
HISTOCOMPATIBILITY 2, CLASS II ANTIGEN A, BETA 1	H2-Ab1	V01527	**-1.3**

Genes are grouped according to their putative functional role. Negative values indicate reduced level of expression in Mel-TG as compared to WT.

1. Gulick J, Subramaniam A, Neumann J, Robbins J. Isolation and characterization of the mouse cardiac myosin heavy chain genes. *J Biol Chem*. 1991;266:9180-5.
2. Vecchione C, Fratta L, Rizzoni D, Notte A, Poulet R, Porteri E, Frati G, Guelfi D, Trimarco V, Mulvany MJ, Agabiti-Rosei E, Trimarco B, Cotecchia S, Lembo G. Cardiovascular influences of alpha1b-adrenergic receptor defect in mice. *Circulation*. 2002;105:1700-7.
3. Brancaccio M, Fratta L, Notte A, Hirsch E, Poulet R, Guazzone S, De Acetis M, Vecchione C, Marino G, Altruda F, Silengo L, Tarone G, Lembo G. Melusin, a muscle-specific integrin beta1-interacting protein, is required to prevent cardiac failure in response to chronic pressure overload. *Nat Med*. 2003;9:68-75.
4. Lembo G, Rockman HA, Hunter JJ, Steinmetz H, Koch WJ, Ma L, Prinz MP, Ross J, Jr., Chien KR, Powell-Braxton L. Elevated blood pressure and enhanced myocardial contractility in mice with severe IGF-1 deficiency. *J Clin Invest*. 1996;98:2648-55.
5. Hilfiker-Kleiner D, Hilfiker A, Fuchs M, Kaminski K, Schaefer A, Schieffer B, Hillmer A, Schmiedl A, Ding Z, Podewski E, Poli V, Schneider MD, Schulz R, Park JK, Wollert KC, Drexler H. Signal transducer and activator of transcription 3 is required for myocardial capillary growth, control of interstitial matrix deposition, and heart protection from ischemic injury. *Circ Res*. 2004;95:187-95.
6. Wolska BM, Solaro RJ. Method for isolation of adult mouse cardiac myocytes for studies of contraction and microfluorimetry. *Am J Physiol*. 1996;271:H1250-5.
7. Kaddoura S, Firth JD, Boheler KR, Sugden PH, Poole-Wilson PA. Endothelin-1 is involved in norepinephrine-induced ventricular hypertrophy in vivo. Acute effects of bosentan, an orally active, mixed endothelin ETA and ETB receptor antagonist. *Circulation*. 1996;93:2068-79.
8. Bonci D, Cittadini A, Latronico MV, Borello U, Aycock JK, Drusco A, Innocenzi A, Follenzi A, Lavitrano M, Monti MG, Ross J, Jr., Naldini L, Peschle C, Cossu G, Condorelli G. 'Advanced' generation lentiviruses as efficient vectors for cardiomyocyte gene transduction in vitro and in vivo. *Gene Ther*. 2003;10:630-6.
9. Brancaccio M, Guazzone S, Menini N, Sibona E, Hirsch E, De Andrea M, Rocchi M, Altruda F, Tarone G, Silengo L. Melusin is a new muscle-specific interactor for beta(1) integrin cytoplasmic domain. *J Biol Chem*. 1999;274:29282-8.

Material and Methods

Generation of transgenic mice

The SalI-BamHI alpha-MHC promoter DNA fragment, obtained from J. Robbins[1], was cloned into SalI-ApaI digested pBluescriptII vector construct containing the myc-tagged cDNA of human melusin followed by β-globin intron and poly-A (Figure 2a). The construct was microinjected in fertilized eggs of FVB mice and transgenic integration was confirmed by southern blot analysis of KpnI digested DNA (Figure 2b) and by PCR analysis, using the following primers: forward CGATATGGAGCAGAAGCTGATC, reverse GATCAGACTGTCAAGTCCTG. The use of animals was in compliance with the guidelines of the European Community and was approved by the Animal Care and Use Committee of the University of Torino.

Transthoracic Echocardiography

Transthoracic echocardiographic analysis was performed in conscious mice using a General Electric System Five Performance cardiac ultrasound machine, equipped with a 10 MHz imaging transducer. Using the 2D parasternal short-axis imaging as a guide, a left ventricular M-mode tracing was obtained in conscious mice. End-diastolic and systolic interventricular septum (IVSTd, IVSTs), posterior wall thickness (PWTd, PWTs) and left ventricular internal diameters (LVEDD, LVESD) were measured using a computed NIH image analysis system. Percent fractional shortening (%FS) and relative wall thickness (RWT) were calculated according to the following standard formulas:

$$\%FS = [(LVEDD-LVESD)/LVEDD] \times 100$$

$$RWT = [(IVSd+PWd)/2]/(LVEDD/2)$$

Reproducibility, calculated as the difference between two determinations divided by the mean of the two determinations and expressed as percentage of error, was 3.5±.5 for LV diameters and 6.9±.8 for wall thickness. Serial echocardiographic evaluations were assessed in mice in basal conditions and during chronic pressure overload (4-8-12 weeks after banding).

Left ventricular haemodynamic

Mice were anesthetized as described[2] with an intraperitoneal injection of tribromoethanol (Avertin, 350 mg/kg) and inotropic and lusitropic function were evaluated by measuring intraventricular volume and pressure with a micromanometer catheter (Millar 1.4 F, SPR 671, Millar Instruments, Inc., USA) positioned in the left ventricle via right common carotid artery canulation[3]. The maximum rate of left ventricular pressure developed (dP/dt max) expressed systolic function, while left ventricular pressure decay (dP/dt min) and time constant of relaxation (τ Glantz) identified diastolic function. The haemodynamic analysis was performed in aortic banded and sham-operated animals after 12 weeks from surgical procedures.

Left ventricular pressure overload

A chronic pressure overload was imposed to the left ventricle through transverse aortic banding (AB) between *truncus anonimus* and left carotid artery, as previously described[3]. To evaluate the degree of pressure overload imposed on the left ventricle, systolic pressure gradient (SPG) was measured by selective cannulation of left and right carotid arteries during the haemodynamic analysis at 12 weeks of aortic banding[4]. A further group underwent the same surgical procedures without aortic stenosis (Sham). After haemodynamic evaluations, the mice were weighted, then the hearts were excised and processed for further molecular analysis.

Conscious blood pressure measurement

Conscious blood pressure and heart rate were measured in unrestrained conditions by a radiotelemetric device (TA11PA-C20, Data Sciences International, St. Paul, MN, USA) whose sensing catheter was inserted into the femoral artery, as previously described[2]. After implantation

mice were housed in a single cage and allowed 10 days recovery from surgical procedures. Blood pressure and heart rate were continuously recorded for 4 hours (from 8:00AM to 12:00AM) for 4 consecutive days. Telemetered pressure signals were stored and analyzed by a dedicated computed data acquisition system (Dataquest Acquisition and Analysis System, DQ ART 1.1 Gold, Data Sciences International, St. Paul, MN, USA) that calculated the mean value during the acquisition time.

Histological analysis

For histological analysis, hearts were fixed with PFA 4% in 20 mM phosphate buffer pH 7,5 overnight at 4°C and paraffin embedded. 5 μm sections were cut at the frontal axis plane. Histological section were stained with hematoxylin/eosin for standard analysis and with Picrosirious red to stain collagen fibers. To quantify fibrosis, whole ventricle slice picture were taken using a 12x stereoscopic microscope and analysis of fibrotic area were performed using ImageProPlus software. Areas of fibrosis were calculated as percentage of total area of the left ventricle. Apoptotic cells were detected by the TUNEL reaction on paraffin embedded heart sections using the TMR red kit (Roche) with no pre-incubation with proteinase K. Nuclei were also counterstained with Hoechst 3342 1μg/ml for 5 min at room temperature. To measure myocyte area and capillary density, suitable cross sections were defined as having nearly circular capillary profiles and nuclei. Capillaries were identified by anti von Willebrand factor antibodies (Sigma) followed by peroxidase labeled secondary antibodies as described[5]. For all quantitative analysis mentioned above, 3 mice for each genotype and 10 histological sections from each heart were analyzed.

Isolation of Adult Cardiac Myocytes and Morphometric Analysis

Cardiac myocytes were enzymatically dissociated from hearts of wild type and melusin over-expressing mice as previously described[6]. Briefly, heart was removed and the aorta was cannulated on a perfusion system. Retrograde perfusion of calcium-free buffer was used to arrest the heart. Heart was, then, perfused with a collagenase-based solution to dissociate myocytes that were plated on laminin-coated substrate after gradual reintroduction of calcium in the presence of 10 mM 2,3-Butanedione Monoxime to inhibit contractility. Two hours after plating, cardiomyocytes were photographed at 20x phase contrast using an inverted microscope and cell areas were measured using ImageProPlus software. Total 100 cardiomyocytes per mouse genotype from four independent experiments were measured.

Northern blot analysis

10 μg of total RNA extracted from left ventricles with the Trizol reagent (Invitrogen) were separated by electrophoresis in 1,5% denaturing formaldehyde agarose-gels and blotted to Hybond nylon membranes (Amersham Biosciences). Membranes were probed with atrial natriuretic factor (ANF) and alpha-skeletal actin (SkA) radiolabeled probes. Band intensities were determined by densitometric analysis from two independent experiments with a total of 6 mice for each genotype.

Embryonic cardiomyocyte isolation and transduction

Ventricular cardiomyocytes were prepared from E19 old Sprague-Dawley rat hearts by enzyme digestion as described[7]. Ventricles were separated from atria and excess vessels and rinsed in 1x ADS solution (116mM NaCl, 20mM HEPES, 0.8mM NaH_2PO_4, 5,4mM KCl, 0,8mM $MgSO_4$, 55mM glucose). Ventricles were cut into four pieces and subjected to a series of digestions with collagenase (type 2, Worthington Biochemical Corporation, Lakewood, NJ) and pancreatin (Sigma) at a concentration of 80.6 units/ml and 62.5 μg/ml, respectively, in 1x ADS solution. Cells were than resuspended in plating medium (4 parts DME and 1 part M199, 10% horse serum, 5% new born calf serum, 100 U/ml penicillin/streptomycin) and seeded in a petri at 37°C for 60 minutes to allow fibroblast adhesion. Non adherent cells were collected and plated onto laminin coated dishes

at the density of $2.5x10^4$ cells in 24-well plates. The final myocyte cultures contained >95% cardiomyocytes as determined by actin staining. After 24 h, medium was changed to maintenance medium (4 parts DME an 1 part M199, 5% horse serum, 0.5% new born calf serum, 100 U/ml penicillin/streptomycin) for the duration of the experiment.
In order to express melusin in these cells, lentiviral vector coding for myc tagged human melusin, and a control vector coding for GFP, were prepared as described[8]. As transfer vector plasmids we used pRRLcPPT.hPGK.MYC-MEL.WPRE and pRRLcPPT.hPGK.GFP.WPRE. These plasmids contains respectively the myc-tagged human melusin gene and the enhanced GFP marker gene driven by the human phosphoglycerate kinase promoter (hPGK). Viral stocks were prepared at 10^6 TU/ml, corresponding to 100 ng p24/ml.
48 h after cardiomyocyte plating, medium was removed and replaced with 1 ml supernatant containing lentiviral vector (100 ng p24) to which 8 μg/ml of Polybrene had been added. Cells were kept overnight at 37°C, washed twice with cold PBS and incubated for 72 h in fresh medium with or without inhibitors indicated below. Infection efficiency was approximately 80% as assessed by GFP fluorescence. To inhibit ERK1/2 and AKT, cells were incubated for 72 h with 50μM MEK-1 inhibitor (PD98059, Calbiochem) or 20μM AKT inhibitor (1L-6-hydroxymethyl-chiro-inositol 2(R)-2-O-methyl-3-O-octadecylcarbonate, Calbiochem). Under these conditions ERK1/2 phosphorylation was inhibited by 85%, while AKT phosphorylation was inhibited by 73% as indicated by western blot analysis with phospho specific antibodies. At the end of the incubation time cells were either fixed and stained with FITC–labeled phalloidin (Sigma) or subjected to western blot analysis as described below.

Western blot analysis

Left ventricles were rapidly dissected, washed in cold PBS and frozen in liquid nitrogen, homogenized with a pestle. Powders were resuspended in 1% Triton X-100, 150mM NaCl, 50mM Tris-HCl pH 8, 1 mM Na_3VO_4, 10 mM NaF, 10 μg/ml leupeptin, 4 μg/ml pepstatin, 0,1 TIU/ml aprotinin), incubated for 1 h at 4°C and centrifuged at 14000 RPM at 4°C to remove debris. Protein concentration was quantified using Biorad and 50 μg samples were separated by SDS-PAGE followed by western blotting. Blots were probed with the following antibodies: antibodies to phospho-Ser9-GSK3β, to phospho-Ser473-AKT, to AKT and to phospho-ERK1/2 were from New England BioLabs; to GSK3β, to ERK1 (C16) and to TGF-β1 were from Santa Cruz Biotechnology; to p38, and to phospho-p38 were from Calbiochem, to Myc epitope and to vinculin from Sigma. The MF-20 monoclonal antibody to myosin heavy chain was obtained from the Developmental Studies Hybridoma Bank. Polyclonal antibodies to melusin were prepared as previously described[9].

Transcriptome analysis

Microarray fabrication: the mouse microarray platform was made with a collection of 13,443 70mer oligonucleotides (Qiagen-Operon, version 1.1). Each oligonucleotide was spotted in two replicates on MICROMAX SuperChip I glass slides (Perkin-Elmer) using Biorobotics Microgrid II (Apogent Discoveries), supplied with 48 stealth micro pins.
RNA purification and labeling: frozen left ventricles were homogenized for 3–5 min using an ultra-turrax-T8 blender (IKA-Werke) in 5 volumes of TRIZOL reagent (Invitrogen/Life Technologies). Total RNA was purified using RNeasy Mini Kit (Qiagen). RNA was subjected to quality control using Agilent Bioanalyzer 2100 (Agilent Technologies). Linear amplification of mRNA from 500ng of total RNA was carried on using the Amino Allyl Message-Amp-aRNA kit (Ambion) with one round of amplification according to the manufacturer's recommendations. 7μg of aRNA from each sample was coupled to Cy3 or Cy5 dyes (Amersham Pharmacia Biotech) to obtain labeled aRNA ready for microarray hybridization.
Microarray hybridization: Labeled RNAs were concentrated by ethanol precipitation and dissolved in 115μl of hybridization buffer (5XSSC, 0.1% SDS, 25% formamide). Labeled aRNA target from wild type and Mel TG heart samples were mixed before precipitation. After denaturation at 90°C

for 2 min, the labeled targets were added to the microarrays, previously incubated in pre-hybridization buffer (5X SSC, 0.1% SDS,100ng/ul ss-DNA, 5X Denhardt) for 2-3 hours at 48°C. Hybridization was carried on overnight at 48°C in an ArrayBooster microarray incubator (Advalytix), followed by a series of post-hybridization washings. Competitive hybridization was done twice using different microarray slides in which each single sample and control RNA was labeled either with Cy3 or Cy5 fluorochromes (dye-swapping procedure). Using this strategy, we obtained four fluorescence intensity values for each probe in the platform. After spot normalization (see below), the average value of probe replicates was calculated. Fluorescence detection was carried out on a GSI Lumonics LITE dual confocal laser scanner (Perkin-Elmer) with ScanArray Microarray Analysis Software, and raw scanner images were analyzed with QuantArray software (Perkin-Elmer). Normalization of the expression levels was performed with MIDAS program (TIGR Microarray Data Analysis System, http://www.tigr.org/software/tm4/). We then performed global and Lowess mean normalizations across element signal intensity and then logarithmic transformation was applied at each expression ratio.

Detection of differentially expressed transcripts: the $\log_2$ expression ratios calculated by MIDAS on each array probe of each competitive hybridization experiment were processed for consistency by the Statistical Analysis of Microarrays software (SAM, http://www-stat.stanford.edu/tibs/SAM/index.html). SAM is a non-parametric statistical test based on a permutation approach specifically implemented for microarray data. On the basis of the SAM output, we chose as threshold level for False Discovery Rate 0.74%. With this value we obtained 110 differentially expressed genes (68 under-expressed and 42 over-expressed in Mel TG versus wild type mice).

Online Table 1. Gene expression profiling of Mel-TG hearts subjected to 12 weeks of AB.

GENE DESCRIPTION	GENE SYMBOL	GenBank ID	EXPRESSION CHANGES
ACTIN, ALPHA, SKELETAL MUSCLE 1	Acta1	M12347	**-2.7**
FIBROSIS			
COLLAGEN, TYPE III, ALPHA 1	COL3A1	X52046	**-2.8**
COLLAGEN, TYPE XV	COL15A1	AF011450	**-2.2**
COLLAGEN, TYPE XIV, ALPHA 1	COL14A1	AJ131395	**-2.2**
COLLAGEN, TYPE VI, ALPHA 3	COL6A3	AF064749	**-1.6**
COLLAGEN, TYPE VI, ALPHA 1	COL6A1	X66405	**-1.9**
COLLAGEN, TYPE I, ALPHA 1	COL1A1	U08020	**-1.6**
COLLAGEN, TYPE V, ALPHA 2	COL5A2	L02918	**-1.9**
PROCOLLAGEN C-ENDOPEPTIDASE ENHANCER 2	PCOLCE2	AK010249	**-1.5**
FIBRILLIN 1	FBN1	L29454	**-1.6**
LUMICAN	LUM	AF013262	**-1.7**
BIGLYCAN	BGN	L20276	**-2.1**
FIBROMODULIN	FMOD	X94998	**-1.4**
SECRETED MODULAR CALCIUM-BINDING PROTEIN 2	SMOC2	NM_022315	**-1.9**
KALLIKREIN 26	Klk26	NM_010644	**+0.7**
LEUKOCYTES/INFLAMATION			
HISTOCOMPATIBILITY 2, CLASS II ANTIGEN A, ALPHA	H2-Aa	NM_010378	**-2.6**
HISTOCOMPATIBILITY 2, O REGION BETA LOCUS	H2-Ob	AF027865	**-2.4**
THYMIC STROMAL-DERIVED LYMPHOPOIETIN, RECEPTOR	Tslpr	AF201963	**-1.7**
IA-ASSOCIATED INVARIANT CHAIN	Ii	X05430	**-1.9**
INTERFERON GAMMA RECEPTOR	Ifngr1	M28233	**-1.5**
CHEMOKINE (C-C MOTIF) LIGAND 21B (SERINE)	Ccl21b	AF001980	**-1.5**
CD14 ANTIGEN	Cd14	M34510	**-1.4**
LYSOZYME	Lyzs	NM_017372	**-1.5**
COMPLEMENT COMPONENT 1, R SUBCOMPONENT	C1r	NM_023143	**-1.4**
CHEMOKINE (C-C MOTIF) LIGAND 21A (LEUCINE)	Ccl21a	U88322	**-1.5**
HISTOCOMPATIBILITY 2, CLASS II ANTIGEN A, BETA 1	H2-Ab1	V01527	**-1.3**

Genes are grouped according to their putative functional role. Negative values indicate reduced level of expression in Mel-TG as compared to WT.

1. Gulick J, Subramaniam A, Neumann J, Robbins J. Isolation and characterization of the mouse cardiac myosin heavy chain genes. *J Biol Chem*. 1991;266:9180-5.
2. Vecchione C, Fratta L, Rizzoni D, Notte A, Poulet R, Porteri E, Frati G, Guelfi D, Trimarco V, Mulvany MJ, Agabiti-Rosei E, Trimarco B, Cotecchia S, Lembo G. Cardiovascular influences of alpha1b-adrenergic receptor defect in mice. *Circulation*. 2002;105:1700-7.
3. Brancaccio M, Fratta L, Notte A, Hirsch E, Poulet R, Guazzone S, De Acetis M, Vecchione C, Marino G, Altruda F, Silengo L, Tarone G, Lembo G. Melusin, a muscle-specific integrin beta1-interacting protein, is required to prevent cardiac failure in response to chronic pressure overload. *Nat Med*. 2003;9:68-75.
4. Lembo G, Rockman HA, Hunter JJ, Steinmetz H, Koch WJ, Ma L, Prinz MP, Ross J, Jr., Chien KR, Powell-Braxton L. Elevated blood pressure and enhanced myocardial contractility in mice with severe IGF-1 deficiency. *J Clin Invest*. 1996;98:2648-55.
5. Hilfiker-Kleiner D, Hilfiker A, Fuchs M, Kaminski K, Schaefer A, Schieffer B, Hillmer A, Schmiedl A, Ding Z, Podewski E, Poli V, Schneider MD, Schulz R, Park JK, Wollert KC, Drexler H. Signal transducer and activator of transcription 3 is required for myocardial capillary growth, control of interstitial matrix deposition, and heart protection from ischemic injury. *Circ Res*. 2004;95:187-95.
6. Wolska BM, Solaro RJ. Method for isolation of adult mouse cardiac myocytes for studies of contraction and microfluorimetry. *Am J Physiol*. 1996;271:H1250-5.
7. Kaddoura S, Firth JD, Boheler KR, Sugden PH, Poole-Wilson PA. Endothelin-1 is involved in norepinephrine-induced ventricular hypertrophy in vivo. Acute effects of bosentan, an orally active, mixed endothelin ETA and ETB receptor antagonist. *Circulation*. 1996;93:2068-79.
8. Bonci D, Cittadini A, Latronico MV, Borello U, Aycock JK, Drusco A, Innocenzi A, Follenzi A, Lavitrano M, Monti MG, Ross J, Jr., Naldini L, Peschle C, Cossu G, Condorelli G. 'Advanced' generation lentiviruses as efficient vectors for cardiomyocyte gene transduction in vitro and in vivo. *Gene Ther*. 2003;10:630-6.
9. Brancaccio M, Guazzone S, Menini N, Sibona E, Hirsch E, De Andrea M, Rocchi M, Altruda F, Tarone G, Silengo L. Melusin is a new muscle-specific interactor for beta(1) integrin cytoplasmic domain. *J Biol Chem*. 1999;274:29282-8.